Supplementary material to

Radical budget analysis in a suburban European site during the MEGAPOLI summer field campaign.

V. Michoud[1], A. Kukui[2,10], M. Camredon[1], A. Colomb[3], A. Borbon[1], K. Miet[1], B. Aumont[1], M. Beekmann[1], R. Durand-Jolibois[1], S. Perrier[1,4], P. Zapf[1], G. Siour[1], W. Ait-Helal[1,5,6], N. Locoge[5,6], S. Sauvage[5,6], C. Afif[7], V. Gros[8], M. Furger[9], G. Ancellet[2], J. F. Doussin[1]

[1] {LISA, UMR-CNRS 7583, Université Paris Est Créteil (UPEC), Université Paris Diderot (UPD), Institut Pierre Simon Laplace (IPSL), Créteil, France}

[2] {LATMOS, UMR-CNRS 8190, Université de Versailles Saint Quentin, Université Pierre et Marie Curie, Guyancourt, France}

[3] {LaMP, UMR-CNRS 6016, Clermont Université, Université Blaise Pascal, Aubière, France}

[4] {ISA, UMR-CNRS 5280, Université Lyon 1, ENS-Lyon, Villeurbanne, France}

[5] {Université Lille Nord de France, Lille, France}

[6] {Department of Chemistry and Environment, Ecole des Mines de Douai, Douai, France}

[7] {Centre d'Analyses et de Recherche, Faculty of sciences, Université Saint Joseph, Beirut, Lebanon }

[8] {LSCE, Université de Versailles Saint Quentin en Yvelines, CEA, CNRS, Gif sur Yvette, France}

[9] {Laboratory of Atmospheric Chemistry, Paul Scherrer Institut, Villigen, Switzerland}

[10] {LPC2E, UMR-CNRS 6115, Orléans, France}

Correspondence to: J. F. DOUSSIN (Jean-Francois.Doussin@lisa.u-pec.fr)

Supplementary material S1: Description of OH and RO_x measurement modes, calibration, estimation of precision and signal corrections.

The reactants used for chemical conversion ($^{34}SO_2$, NO and NO_2) are injected into the reactor through a set of injectors. Switching the reactant flows between the different injectors allows measurements in four different modes: a background mode, two different OH radical measurement modes and a RO_2 radical measurement mode. The two OH measurement modes differ by the time used for the chemical conversion (see below). OH, RO_2 and H_2SO_4 measurements were performed by monitoring the peak intensities at m/z = 62 (NO_3^-), m/z = 99 ($H^{34}SO_4^-$) and m/z = 97 ($H^{32}SO_4^-$). The detection of $H^{34}SO_4^-$ and $H^{32}SO_4^-$ corresponds to the measurement of OH (or RO_2) and ambient H_2SO_4, respectively. Typically, 1 min measurements for each OH or background detection mode consisted of 25 samples of 1 s at m/z = 99 (OH) and 25 samples of 1s at m/z = 97 (H_2SO_4). Every 2 min OH measurements included a 1 min OH signal and two 30 s background signals on both sides of the OH signal. An OH detection sequence comprises 3 to 6 of OH measurement cycles of 2 min. At the end of each OH detection sequence NO was switched to the corresponding injector for the measurement of RO_2, typically for 1 min. For several periods the RO_2 measurements were interrupted and the OH measurements were performed without addition of NO into the reactor. No difference could be detected for the OH detection with NO or without it.

Calibration of the instrument was performed with a previously described calibration cell [Kukui et al., 2008]. The calibration is based on production of controlled concentrations of OH and RO_2 radicals in a turbulent flow reactor by photolysis of water vapour at 184.9 nm [Heard and Pilling, 2003 and references herein; Faloona et al., 2004; Dusanter et al., 2008]. The concentration of the radicals generated in the turbulent flow is calculated from the monitored photon flux and measured humidity. The ion peak intensities detected at m/z = 62 (I_{62}) and m/z = 99 (I_{99}) corresponding to the NO_3^- and $H^{34}SO_4^-$ ions are related to the concentrations of radicals R (R = OH or HO_2) produced in a calibration unit by the following equation:

$$[R] = CR \times \ln (1 + I97 / I62) \quad (1)$$

The calibration coefficients C_R can be derived from the estimated concentrations of radicals produced in the flow tube, [R], and the measured I_{97}/I_{62} ratio.

The overall accuracy of the calibration coefficients is estimated taking into account uncertainties of all parameters used for calculation of the radical concentrations and the precision of the I_{97}/I_{62} measurements [Kukui et al., 2008]. The main source of the calibration uncertainty comes from the accuracy of estimation of the photon flux inside the reactor depending in particular on the uncertainty of phototube sensitivity. The uncertainty (2σ) of the OH calibration coefficient C_{OH} has been estimated to be 30%.

The calibration of HO_2 and CH_3O_2 was performed by adding CO or CH_4 into the calibration cell photolysis reactor, converting OH to HO_2 or CH_3O_2, respectively [Hanke et al., 2002; Fuchs et al., 2008]. The HO_2 calibration coefficient was found to be 15% higher than that for the CH_3O_2. The total peroxy concentration was calculated with the calibration coefficient average between HO_2 and CH_3O_2, assuming that these radicals represented the major part of the total peroxy radicals with approximately equal contribution. Accounting for an uncertainty in the RO_2 composition, the calibration uncertainty (2σ) for the RO_2 measurements is estimated to be 40% under MEGAPOLI conditions.

Precision of the OH and RO_2 measurements was estimated from the signals statistics during the calibration measurements. For the 10 min averaged data the precision corresponding to a standard random deviation was better than 10% for OH concentrations higher than 10^6 molecule cm^{-3} and better than 5% for RO_2 levels higher than 10^8 molecule cm^{-3}.

Accounting for the measurement precision and the calibration uncertainty estimated from the calibration measurements performed 4 times during the MEGAPOLI campaign, the overall (2σ) uncertainty of the 10 min averaged measurements of OH and HO_2+RO_2 is estimated to be 35% and 45%, respectively. The detection limit of 8×10^5 molecule cm^{-3} for one 2 min OH point was calculated from the signal statistics in background mode at a signal to noise ratio of 3.

During the MEGAPOLI campaign rather high NO levels, up to 20 ppb, were encountered. Under such conditions the OH measurements could be significantly influenced by a contribution from the OH radical formed in the CCR via reaction of ambient HO_2 and NO [Kukui et al., 2008]. The correction for this effect was made from a difference of the OH signals measured using the “long” and the “short” modes (in preparation, will be submitted to Atmos. Meas. Tech.). For most of the OH data the correction was less than 15%, but sometimes under conditions of high NOx it was as high as 35%. The correction for the artificial OH formation added on average less than 5% to the overall OH measurements uncertainty (2σ).

Supplementary material S2: Analysis of the estimation of unmeasured secondary VOCs by the different versions of the model

To compare the measured secondary VOC with estimates made with the MCM model using different scenarios, simulations have been performed by removing the Methyl-Vinyl Ketone (MVK) constraints. The results of these simulations are shown in Fig. S2. The MVK has been chosen because it usually represents a secondary product with no significant primary sources and has a long lifetime (approximately 20h with OH [ ]) and thus is a good target species. The concentrations simulated with the various versions of the model match the order of magnitude of the observed concentrations. However, no model version captures the measured daily profile. The best model version can hardly be identified. However, the test shows that the different model versions encompass non measured secondary species most of the times.

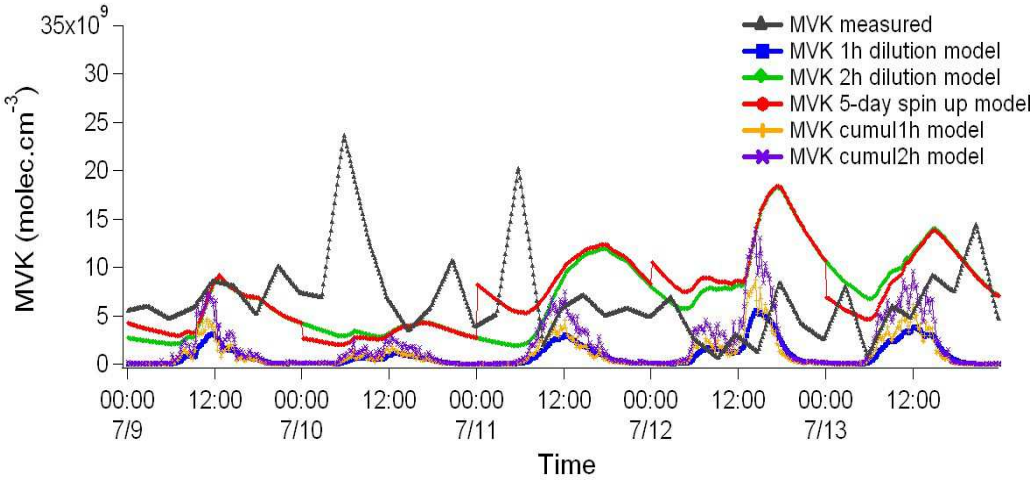

Figure S2: Observed [MVK] concentrations (black triangles) compared to concentrations simulated with the three model versions used in this study: dilution model with corresponding time of 1h (blue squares) and 2h (green diamonds) for the dilution loss terms, 5-day spin up model (red circles) and model with 1h (orange plusses) or 2h (purple crosses) accumulation for each 10 min time for the secondary unconstrained species.

Supplementary material S3: Discussion on the correlation between OH and J(O^1D)

As discussed in the section 4.1 of the article, the averaged diurnal variations of OH and J(O^1D) show very similar behaviour. To quantify this relationship, the correlation between OH and J(O^1D) is shown in Fig. S3. As expected, a good correlation (R^2 = 0.62) was found

between OH and $J(O^1D)$. This correlation does not describe the direct dependency of OH on photolysis frequency of ozone to O^1D but much more the general dependency of OH on photolytic processes such as the photolysis of O_3 but also the photolysis of HONO, HCHO or other aldehydes [Ehhalt and Rohrer, 2000; Holland et al., 2003]. The determination coefficient R^2 is consistent with other studies [Creasey et al., 2001; Ren et al., 2005]. Better correlations were found in rural environments during BERLIOZ [Holland et al., 2003] and during a field campaign on an unpolluted site in northeastern Germany [Ehhalt and Rohrer, 2000] with correlation coefficient R^2 up to 0.8. In their analysis of OH data, Smith et al. (2006) found that a power-dependence upon $J(O^1D)$, of the form $OH = a\ J(O^1D)^b$, resulted in a better fit than a simple linear expression because the exponential parameter b incorporates the influence of different photolytic OH sources including $J(NO_2)$ or J(HONO). In our case, no significant improvements of the correlation were found; R^2 being 0.62 for a linear expression and 0.65 for a power expression.

The slope of this correlation from a linear regression fit is 1.94×10^{11} s^{-1} cm^{-3} for this study which is very close to the slope found during the BERLIOZ campaign [Holland et al., 2003] although approximately twice lower than Ehhalt and Rohrer (2000) during the POP-CORN campaign (3.94x1011 s^{-1} cm^{-3}), both campaigns conducted in rural sites.

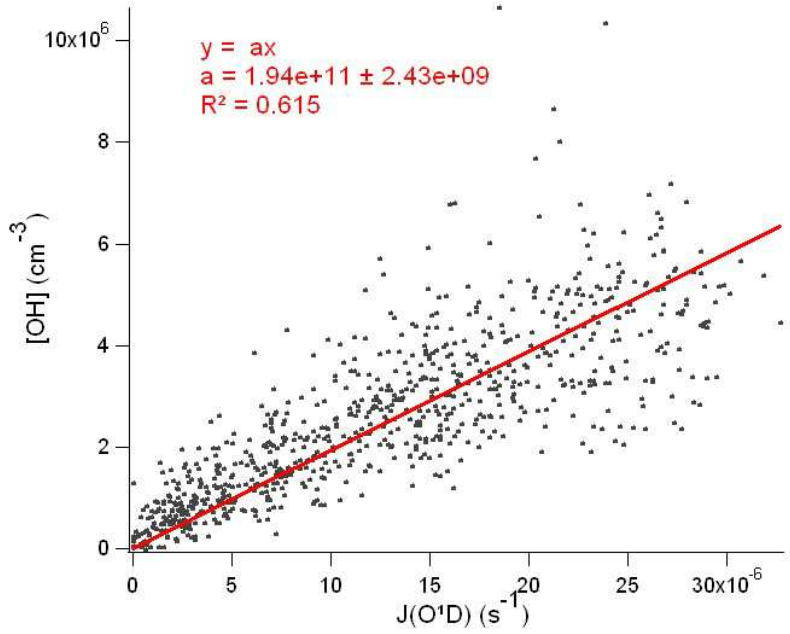

Figure S3: Correlation between OH and $J(O^1D)$ during MEGAPOLI summer campaign, 09-26 July 2009. The correlation coefficient R^2 is 0.615 for the full data set of the studied period.

Supplementary material S4: Variation of the modelled/measured OH concentration ratio with NO_x concentrations

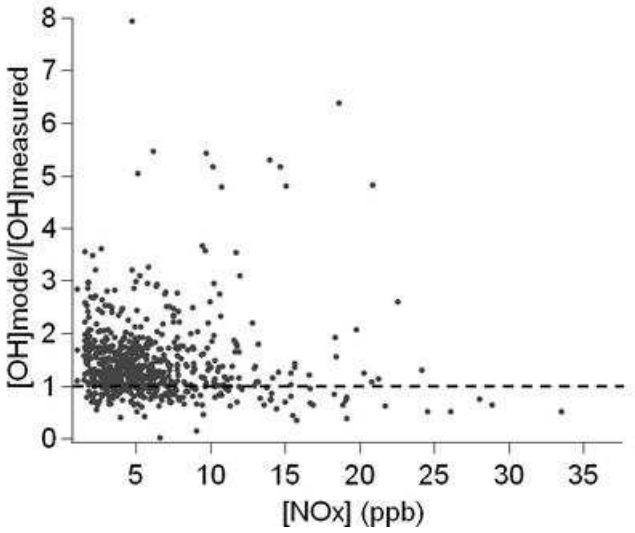

Figure S4: Variation of the ratio between modelled (with the 5-day spin up model version) and measured OH concentrations versus NO_x concentrations in ppb. The dotted line represents a ratio between modelled and measured OH concentrations of 1.

Supplementary material S5: Effect of the HO_2 and CH_3O_2 uptake on aerosol surfaces on simulated OH and RO_2 concentrations

Simulations have been run adding an uptake of HO_2 and CH_3O_2 on aerosol surface to the 5-day spin up model. Owing to the short lifetime of OH (~1s), its uptake on aerosol surface is unlikely to affect its concentrations even with $\gamma = 1$ [Jacob, 2000], thus we have added only heterogeneous uptake of HO_2 and CH_3O_2 in the model which exhibit longer lifetimes. The heterogeneous uptake of these species is simulated using the free molecular approach described in [Sommariva et al., 2006]:

$$K_{het} = \frac{Ac\gamma}{4} \quad (2)$$

Where A is the aerosol surface area, c is the mean molecular speed (cm s^{-1}) and γ is the reaction probability. The aerosol surface area was calculated using Aerosol Particle Sizer (APS) data. This instrument was deployed by the Paul Scherrer Institute team at the SIRTA observatory during the MEGAPOLI summer campaign. The mean aerosol surface area during the study period was $2.3.10^{-7}$ cm^2 cm^{-3}. The reaction probability γ_{HO2} is known to be

comprised in the range 0.1-1 [Jacob, 2000]. However, a recent study found γ_{HO2} less than 0.01 for H_2SO_4 aerosols [Thornton and Abbatt, 2005]. We used two different values for the model parameterization: 0.2 which is the value recommended in [Jacob, 2000] and 1 which is the theoretical maximum. The reaction probability γ_{CH3O2} used in the model was 3.10^{-3} [Gershenzon et al., 1995].

Under the conditions encountered during the MEGAPOLI summer campaign, the addition of HOx uptake on the aerosol surface in our model does not lead to a significant improvement of the simulated radical concentrations. The results of the model with the new scenarios compared with the measurements are shown in Fig. S5 and the changes observed in the simulated radical concentrations are shown in Fig. 13 in the article. Indeed, the major effect was seen in predicted HO_2 concentrations with a reduction of 0.2% and 1.1% for a reaction probability γ_{HO2} of 0.2 and 1 respectively. The reduction of predicted OH and RO_2 concentrations were less important with only 0.1% and 0.4% for both OH and RO_2 for a reaction probability γ_{HO2} of 0.2 and 1 respectively. Thus, these decreases caused by the addition of heterogeneous radical uptake in our model by far cannot resolve the overestimation of simulated OH and RO_2 concentrations, since the aerosol surface area was probably too small.

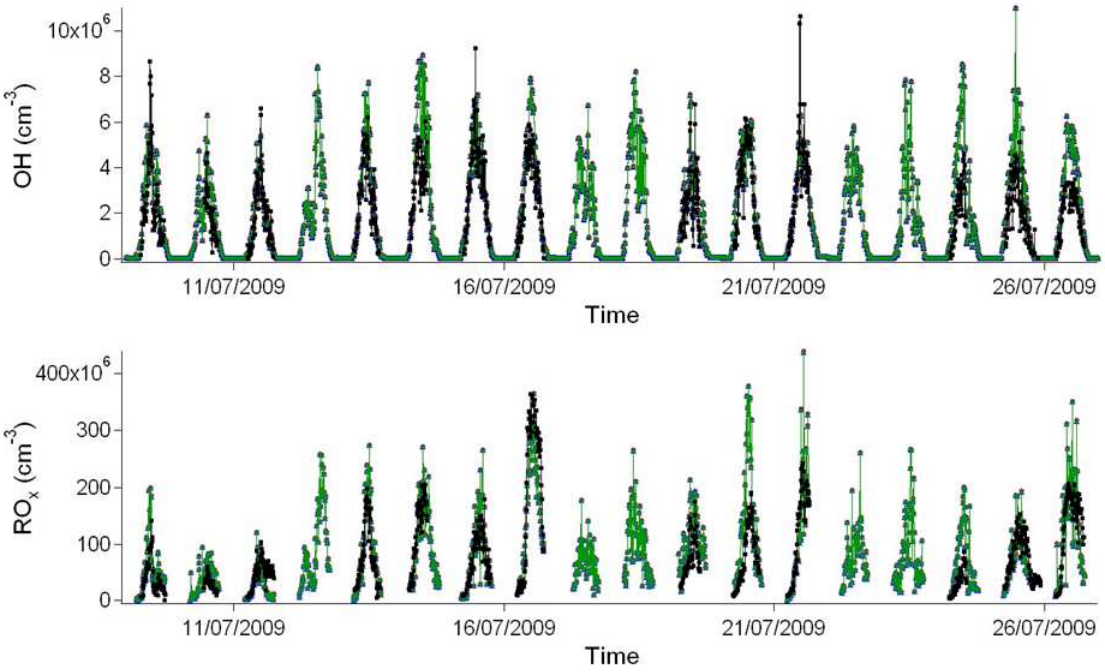

Figure S5: Effect of heterogeneous uptake addition on OH and RO_2 concentrations. Black squares represent the measurement, red circles represent the reference model, blue triangles represent the base model + heterogeneous uptake with a reaction probability of 0.2 for HO_2

uptake and green diamonds represent the base model + HO_x heterogeneous uptake with a reaction probability of 1 for HO_2 uptake. Because results are very similar, the red, the blue and the green curves are difficult to discern.

References

Cox, R. A., Derwent, R. G., and Williams, M. R.: Atmospheric photo-oxidation reactions. Rates, reactivity, and mechanism for reaction of organic compounds with hydroxyl radicals, Environmental Science & Technology, 14, 57-61, 1980.

Dusanter, S., Vimal, D., and Stevens, P. S.: Technical note: Measuring tropospheric OH and HO2 by laser-induced fluorescence at low pressure. A comparison of calibration techniques, Atmos. Chem. Phys., 8, 321-340, 2008.

Ehhalt, D. H., and Rohrer, F.: Dependence of the OH concentration on solar UV, J. Geophys. Res., 105, 3565-3571, 2000.

Faloona, I. C., Tan, D., Lesher, R. L., Hazen, N. L., Frame, C. L., Simpas, J. B., Harder, H., Martinez, M., Di Carlo, P., Ren, X. R., and Brune, W. H.: A laser-induced fluorescence instrument for detecting tropospheric OH and HO2: Characteristics and calibration, J. Atmos. Chem., 47, 139-167, 2004.

Fuchs, H., Holland, F., and Hofzumahaus, A.: Measurement of tropospheric RO(2) and HO(2) radicals by a laser-induced fluorescence instrument, Rev. Sci. Instrum., 79, 2008.

Gershenzon, Y. M., Grigorieva, V. M., Ivanov, A. V., and Remorov, R. G.: O-3 and OH sensitivity to heterogeneous sinks of HOx and CH3O2 on aerosol particles, Faraday Discussions, 100, 83-100, 1995.

Hanke, M., Uecker, J., Reiner, T., and Arnold, F.: Atmospheric peroxy radicals: ROXMAS, a new mass-spectrometric methodology for speciated measurements of HO2 and Sigma RO2 and first results, International Journal of Mass Spectrometry, 213, 91-99, 2002.

Heard, D. E., and Pilling, M. J.: Measurement of OH and HO2 in the troposphere, Chem. Rev., 103, 5163-5198, 2003.

Holland, F., Hofzumahaus, A., Schafer, R., Kraus, A., and Patz, H. W.: Measurements of OH and HO2 radical concentrations and photolysis frequencies during BERLIOZ, J. Geophys. Res., 108, 2003.

Jacob, D. J.: Heterogeneous chemistry and tropospheric ozone, Atmospheric Environment, 34, 2131-2159, 2000.

Kukui, A., Ancellet, G., and Le Bras, G.: Chemical ionisation mass spectrometer for measurements of OH and Peroxy radical concentrations in moderately polluted atmospheres, J. Atmos. Chem., 61, 133-154, 2008.

Ren, X. R., Brune, W. H., Cantrell, C. A., Edwards, G. D., Shirley, T., Metcalf, A. R., and Lesher, R. L.: Hydroxyl and peroxy radical chemistry in a rural area of Central Pennsylvania: Observations and model comparisons, J. Atmos. Chem., 52, 231-257, 2005.

Sommariva, R., Bloss, W. J., Brough, N., Carslaw, N., Flynn, M., Haggerstone, A. L., Heard, D. E., Hopkins, J. R., Lee, J. D., Lewis, A. C., McFiggans, G., Monks, P. S., Penkett, S. A., Pilling, M. J., Plane, J. M. C., Read, K. A., Saiz-Lopez, A., Rickard, A. R., and Williams, P. I.: OH and HO2 chemistry during NAMBLEX: roles of oxygenates, halogen oxides and heterogeneous uptake, Atmos. Chem. Phys., 6, 1135-1153, 2006.

Thornton, J., and Abbatt, J. P. D.: Measurements of HO2 uptake to aqueous aerosol: Mass accommodation coefficients and net reactive loss, J. Geophys. Res., 110, 2005.